Optical Engineering

OpticalEngineering.SPIEDigitalLibrary.org

Soil signature simulation in the thermal infrared

Tyler Carson
Carl Salvaggio

SPIE.

Soil signature simulation in the thermal infrared

Tyler Carson* **and Carl Salvaggio**
Chester F. Carlson Center for Imaging Science, Rochester Institute of Technology, Digital Imaging and Remote Sensing Laboratory, 54 Lomb Memorial Drive, Rochester, New York 146230, United States

Abstract. Soil emissivity signatures were constructed using the digital imaging and remote sensing image generation (DIRSIG) model and Blender three-dimensional (3-D) graphic design software. Using these tools, the geometry, radiometry, and chemistry of quartz were exploited to model the presence of particle size effects in the thermal spectra of disturbed soil. Using the physics engines within the Blender 3-D graphic design software, a physical representation of a granular soil scene was created. Chemical and optical properties of pure quartz were assigned to particles in the scene based on particle size. The spectral signature of disturbed soil was modeled by the physical mixture of small fine particles (50 μm diameter) and larger grains (500 μm diameter). The study demonstrated that by combining realistic target geometry and spectral measurements of pure quartz, emissivity of complex soil mixtures could be modeled without functional data fitting or rigorous analysis of material dynamics. [DOI: 10.1117/1.OE.54.10.104102]

Keywords: reststrahlen; spectral contrast; emissivity; infrared; hyperspectral.

Paper 150624 received May 13, 2015; accepted for publication Sep. 14, 2015; published online Oct. 6, 2015.

1 Introduction

It is often desired to pinpoint the scattering signatures of radiation that vary from target to target. Many samples of interest are made of material mixtures. This means that the spectral or thermal signature of a specimen of interest will likely contain intimate combinations of various geometries and material properties. This complication makes modeling difficult.

The complex target considered in this work is quartz-based soil. Thermal infrared spectra of powdered and granular quartz have been studied in order to define the hyperspectral remote sensing characteristics of buried landmines[1–3] and planetary bodies.[4] The disturbed soil that accompanies the placement of landmines possesses a thermal signature that is transient.[1] Although the optical properties of a surface may not change over time, a burial site is exposed to weather, which alters the geometric configuration of soil particulates.[5] Very fine particles that electrostatically cling to larger grains contribute largely to soil signatures. As sand is washed by dew or packed by winds, the forces that bond the fines and grains together are overpowered. Fines get rinsed or blown away and the particle size distribution of the sensed sample is changed. We propose that in order to effectively model disturbed soil, the geometric particle distributions that define spectral characteristics must be physically represented.

1.1 *Phenomenology*

Soil particles consist mostly of rock-forming minerals. In the presence of external forces and charges, the ionic bonds that make up these minerals will stretch and vibrate. Fundamental molecular vibrations are known as reststrahlen, and the acoustical features that are present in the spectral emissivity signatures of quartz-based soil are called reststrahlen bands. These bands correspond to a sudden decrease in emissivity. Two notable reststrahlen band emissivity troughs can be sensed between 7.5 and 10 μm.

It is the magnitude of the reststrahlen emissivity troughs that can be used as target identifiers. Even when quartz is a minority component within a mixture, quartz reststrahlen bands tend to dominate the shape of the corresponding spectral curves.[6] The addition of other minerals has a broadening effect upon the emissivity troughs. It should also be noted that both the magnitude and shape of the reststrahlen bands are impacted by the variety and color of quartz that is measured.

Spectral contrast is another identifiable feature observed in the hyperspectral description of soils. With respect to quartz-based sand, this contrast refers to the height of the emissivity peak that separates the two notable emissivity troughs in the 7.5–10 μm region of the long-wave infrared (LWIR) spectrum. In 1964, Lyon observed that the spectral contrast in this wavelength regime was dependent upon particle size.[7] Further, contrast tends to decrease with decreasing particle size. Salisbury and Wald proposed that the dominating volume scatter of optically thin grains is the primary impetus for reduced spectral contrast within the reststrahlen region.[8] He also explained the indirect link between contrast and the porosity of granular soil targets. Soils with high levels of porosity allow for the incoherent scattering of individual quartz particles, and exhibit higher emissivity and less contrast than do closely packed sand samples. Additional observations by Johnson et al.[1] affirmed the relationship between soil emissivity and porosity. Bachmann et al. highlighted the difficulties surrounding the inclusion of porosity and particle size effects within physical reflectance models.[9] It has been shown here that geometry certainly impacts the ability to discern between soil targets. Prior to this work, the geometric aspects of particle shape, size, and spacing have not been adequately integrated into a model to predict complex soil signatures.

*Address all correspondence to: Tyler Carson, E-mail: tdc9005@rit.edu

Soil emission phenomenology cannot be thoroughly discussed without acknowledging the influence of material chemistry. In the 7.5–10 μm regime, optical properties of quartz vary. Moersch and Christensen explain that due to the high imaginary component of the complex index of refraction, specular Fresnel reflections dominate the spectral region defined by the reststrahlen emissivity troughs.[10] Because of these reflections, thermal energy cannot easily propagate through soil grains in a medium. Stifled radiation transport in this spectral region leads to the formation of emission troughs. This effect poses an interesting modeling problem. The optical properties of large quartz particles and tiny quartz particles are the same. Yet, small quartz particles display much higher emissivity than larger grains of the very same material. Moersch and Christensen explain that the likelihood of emission from particles depends on the coupled relationship between particulate geometry and chemistry. Radiation within a small particle will interact with the grain boundary more frequently before reabsorption than will radiation in a larger particle (Fig. 1).

Therefore, radiation within smaller particles has a greater chance of being emitted and propagated to a sensor at certain wavelengths. In this specific trade-space of geometry and chemistry, geometry seems to impact the detectability of the signature most. We do not presume to say that the optical properties of quartz in this region do not contribute to the presence of emission troughs. We only contend that the spectral identifiers of emissivity magnitude and spectral contrast are spawned from a dependent relationship.

1.2 *Modeling Phenomenology*

This discussion has named several of the subprocesses that are associated with radiation scatter and emission. A true description of scatter should include each and every physical trait that contributes to reflection and emission. Omission of phenomenology leads to false attribution of physical effects within a model. The result is a tool that may be force fitted to describe a target with accuracy. Such an algorithm may not be invertible. It would produce an unphysical result for other samples that scatter light differently. Surely, the failure to include necessary scattering parameters makes simulation difficult. Presuming all physical scatter contributions could be included, modeling them all in parallel is a daunting task. This would likely require many different properties to be specified and not every parameter can be independently modeled. This is why appending physical considerations to existing models should be done with care.[11,12] Important relationships between geometric, radiometric, and chemical parameters must be acknowledged. If certain parameters are underestimated or incompletely described in an algorithm, there exists a need for unphysical scaling factors.[11]

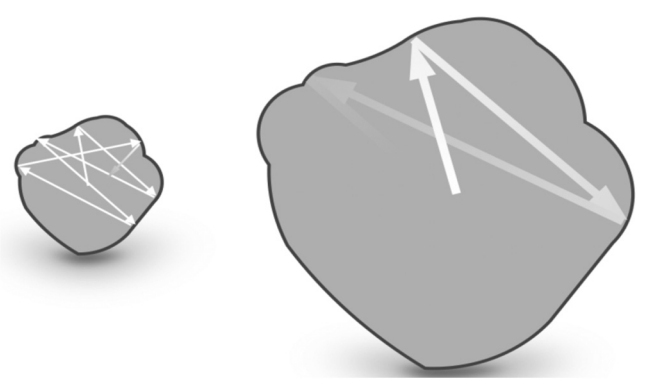

Fig. 1 Prereabsorption interactions between thermal radiation and grain boundaries depend on particle size. When compared to small particles, radiation emitted from large grains travels a longer optical path to experience the same number of radiation-boundary interactions.

1.3 *Modeling with Digital Imaging and Remote Sensing Image Generation and Blender Three-Dimension*

It is important to state what this model is not. The method described in this paper is not an attempt to explicitly solve for all physical and chemical phenomenology associated with the reflection and emission of complex soils. It is not a parameter-based model containing arbitrary functions that are fit to data curves. This procedure will not approximate surface geometry as a probabilistic distribution of facets.[12] It does not presume that a surface of thousands of irregular particles will scatter as a linear combination of individual phase functions solved independently of one another.[11]

This is a method focused on scene geometry that simulates the reflectance and emissivity of complex mixtures of solids. This is an avenue to explore the phenomenology of particle size distribution, density, and intimate mixing. Most importantly, the model bundles together the chemical, radiometric, and geometric components of material signatures.

Chemical parameters to be considered in a soil scattering model include indices of refraction, absorption, anomalous dispersion, anisotropy, and lattice vibrations. Solving for each of these constraints is very difficult. Instead, measured emissivity spectra of pure materials are used in this simulation procedure. For instance, soil particles in this model that possess a 50 μm radius are attributed with the emissivity spectra of 50 μm soil.

The radiometric aspects of this simulation are solved using the DIRSIG model. DIRSIG is a first principle-based ray-tracing model that produces at-sensor radiance.[13,14] Light sources, scene geometries, and sensor configurations are all defined by the user (Fig. 2). This model has been predominantly used for the analysis and modeling of sensors. DIRSIG allows for direct system comparisons. A single scene can be observed under varying

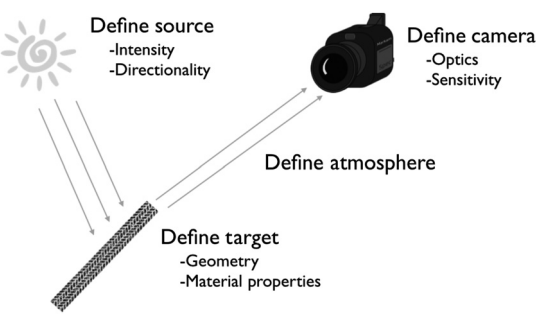

Fig. 2 The versatility of digital imaging and remote sensing image generation (DIRSIG) lies in user control. Within a single simulation, each link of the imaging chain can be modeled with precision. The input of the chain is a uniquely defined scene and irradiance level. The output is a radiance image produced by a virtual sensor. Links of the chain include the light source, radiation propagation, target geometry, atmosphere, and the sensor. Parameters of each link are defined prior to simulation. Since the model is compartmentalized, scenarios can be changed with precision and with ease.

atmospheric conditions, with multimodal sensing techniques. Though it is easy to conceptualize passive remote sensing as light rays traveling from source to target to sensor, DIRSIG models radiation in inverse fashion, using backward ray tracing. Rays are initially cast from individual pixels of a user-defined focal plane array. These rays determine what each pixel sees and where radiation originates.

The geometry of soil is created using the Blender three-dimensional (3-D) open source graphic design software. This design suite gives users the ability to etch, bend, and connect different shapes or planes to create objects with precision. Using built-in physics engines, one can create a scene of objects that interact based on the physical properties (mass and shape) defined by the user. Simulating rigid body collisions, fluid motion, and force field interactions is all possible using the Blender 3-D tool. Each mesh object is subjected to friction and damping, and interacts with other objects through collisions based on mass. Individual mesh facets influence collisions between in-scene objects. This implies that a convex hull does not define the physical bounds of a soil particle created in Blender 3-D. For instance, a multifaceted particle is bounded by its facets rather than a sphere or a six-sided cube with similar volume.

2 Methods

2.1 *Geometry*

This model of disturbed soil begins with a geometric description at the microscopic scale. As alluded to the introduction, mesh objects of different geometries are rotated, translated, and extruded to produce objects that match the 3-D geometry of soil grains. Scanning electron microscope (SEM) images provided a visual template for particle design. An example image can be seen in Fig. 3.

In previous discussion, it was explained that weathering and human disturbance contribute to the distribution of different particle sizes within a target sample. It was observed that small fine particles cling to larger soil particles when the ground soil is sifted or dug up and overturned.[1,8] The presence of the fine dusting, combined with altered porosity, distinctly changes the magnitude and shape of sample spectral signatures. The scene built to model disturbed soil included superfine dust grains clinging to larger sand or soil particles. Two separate shapes with average diameters of 60 μm and 35 μm were used to represent fine dust particles. Three other shapes represented large grains. These three particles had average diameters of 500 μm, 640 μm, and 853 μm, respectively. Each of the five shapes was created manually using SEM imagery as a template. In Blender 3-D, a dusty sand particle was created through a simple process. First, a large grain particle (500 to 853 μm) was designed. Then a multitude of superfine particles was formed. Next, the facets of the large grains were subdivided into smaller facets that have a diameter that is close in size to the dusty fines. By manually aligning particle faces, each piece of dust was easily abutted to the larger particle. A parent–child relationship was set between the large grain and the fine particulates. This ensured that the large grain and the dust grains remained in contact during rigid body simulation. This also allowed for grains of each size to be assigned their own unique material spectra before the final geometry was exported to DIRSIG. A Blender 3-D representation of a dusty particle is depicted in Fig. 3.

Realistic scene posing and mixing were performed using the Blender 3-D physics engine. To model a natural soil scene, particles were not individually placed by hand. User placement of thousands of objects would be incredibly tedious and likely unphysical. Each particle was treated as a rigid body and was dropped onto a surface where particle interactions occurred. Grains eventually settled into a physical 3-D soil scene. This process is illustrated in Fig. 4.

In the graphic design software, this soil scene simulation takes the form of a motion picture. At each frame, particle position was calculated using the mass, shape, and external forces of gravity and inter-particle collisions. A single frame was used as the target description within the DIRSIG radiometry solver. This geometry included the position in x, y, z coordinates of all object vertices. It is an actual record of particle shape and position that forms an accurate account of particle distribution and spacing.

2.2 *Chemistry*

Before the soil grains were inserted into a DIRSIG radiometry simulation, emissivity spectra were assigned to the facets of each particle. Spectral reflectance and emissivity response curves represent how each facet will respond to

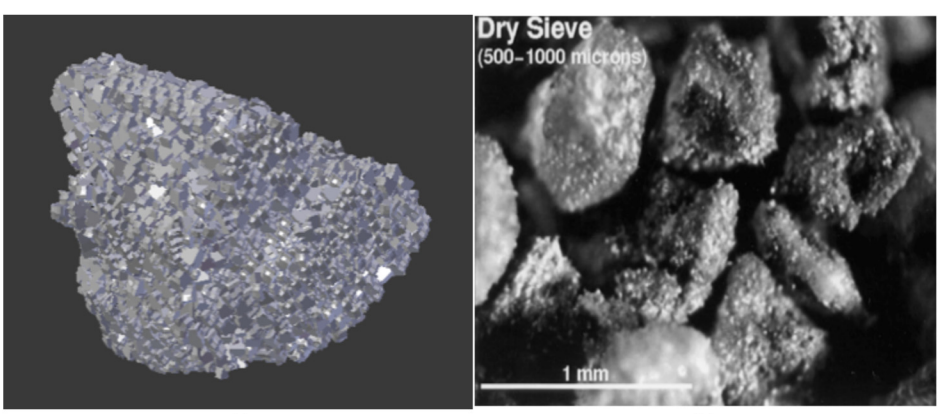

(a) (b)

Fig. 3 (a) A soil particle covered in dust grains is one example of precise geometric modeling that is native to Blender three-dimension. (b) Scanning electron microscope images reveal small dust particles clinging to larger grains.[1]

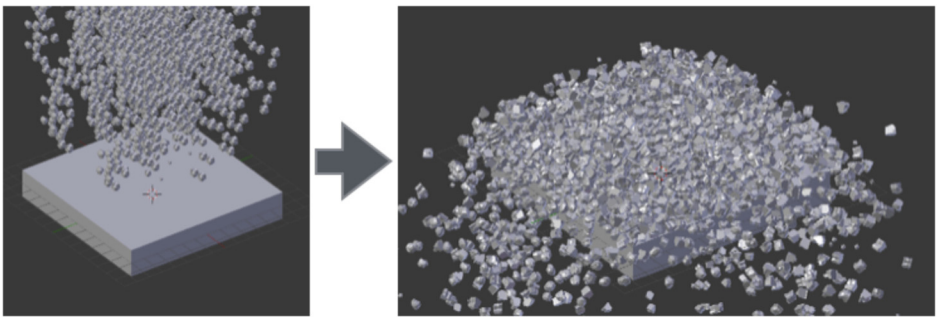

Fig. 4 The process of scene building is based upon physics engines in Blender 3-D. Above, particles fall onto a surface where they settle naturally in space. A video of this process can be viewed online.[15]

interaction with a photon. It is known that large and small quartz particles have distinct LWIR spectra due to the incoherent emission of radiation.[8] The directional hemispherical reflectance spectra of quartz have been published for many specific size distributions (including 50 μm grains).[1,16] These data were extracted and converted into DIRSIG emissivity files.

2.3 *Radiometry*

Radiance that is measured by a DIRSIG imager or a laboratory sensor has multiple components. Radiation leaves a target to be detected through the processes of reflection (L_r) and emission (L_e). Radiance upwelling (L_u) from the ground/target plane is a linear combination of these two processes

$$L_u(\lambda) = L_e(\theta_r, \phi_r, \lambda) + L_r(\theta_r, \phi_r, \lambda). \tag{1}$$

To know target emissivity, the emissive and reflective components of Eq. (1) must be separated. Empirical methods used to separate these terms are nontrivial. To calculate emissivity, downwelling radiance (L_d) must be known or measured. Downwelling radiance is the radiation from the sky or a light source that illuminates a target. The equation used in DIRSIG and in the laboratory to find spectral emissivity is

$$\varepsilon_{\text{target}}(\lambda) = \frac{L_{\text{target}}(\lambda) - L_d(\lambda)}{L_{\text{BB}}(\lambda, T_{\text{target}}) - L_d(\lambda)}. \tag{2}$$

L_{target} describes the radiance measured from a target by a DIRSIG sensor. Temperature-dependent blackbody radiance (L_{BB}) refers to radiance calculated according to Planck's law. Note that the temperature used to calculate blackbody radiance must match that of the sample if correct emissivity is to be derived.

Obtaining emissivity using Eq. (2) is a conditional process.[17] When the temperature of the downwelling atmosphere is similar to that of the target, there is little contrast between values in the numerator of Eq. (2). This results in small emissivity values that may be dominated by noise. Also, if the values in the denominator of Eq. (2) have similar magnitudes, the emissivity equation becomes unstable. For these reasons, performing good emissivity measurements in the field or laboratory is hard to do. On very clear days, downwelling radiance (L_d) is relatively stable and the sky is usually much colder than the sample of interest. In this scenario, Eq. (2) provides good results. When conditions are imperfect, the sample temperature and the atmospheric temperature are knowingly altered in experimental situations in order to increase the contrast between radiance values. The accuracy of the emissivity results also depends on how well the temperature of the sample is known. Temperature emissivity separation and curve smoothing techniques are often employed to find actual temperatures from a selection of probable temperatures.[18]

Using DIRSIG to simulate emissivity data does require some experimental manipulation, but the process is relatively easy and does not call for the postprocessing described above. Users have control of in-scene radiance sources. By removing these sources, the downwelling radiance (L_d) term in Eq. (2) is nullified and a simple ratio remains

$$\varepsilon_{\text{target}}(\lambda) = \frac{L_{\text{target}}(\lambda)}{L_{\text{BB}}(\lambda, T_{\text{target}})}. \tag{3}$$

DIRSIG allows in-scene objects to be attributed with a specific temperature. This implies that the user can define the temperature of an object, and blackbody radiance (L_{BB}) is completely known. The user's control of radiation sources and temperature allows for emissivity to be solved painlessly.

With this theory in mind, the process to create emissivity simulations can be defined. First, import geometry into DIRSIG using. obj files. These files contain the locations of all the vertices and edges of objects in the target scene. Next, multiple instances of target geometry are defined within a. odb file. This allows for the size of a target to be expanded. Material (.mat) files are configured to link temperature and wavelength-dependent spectral properties to facets in the scene. In this study, a temperature of 300 K was used to define target radiance and blackbody radiance. To impose the conditions of Eq. (3), irradiance from the in-scene light source is set to zero. This parameter is set within the atmosphere (.atm) file. Last, sensor geometry and response are defined. The sensor used in simulation must be configured within the platform file to be responsive in the desired wavelength range. A spectral resolution of 10 nm was used in this work.

Using the scenes and modeling techniques described above, the LWIR soil signatures in the reststrahlen bands can be modeled. Emissivity can be found for a sample of disturbed soil. DIRSIG provides user control of temperature and source radiance, which allows for reflection and emission to be evaluated separately. This process provides a method to simulate *in situ* soil signatures. Recreation of such scenes is difficult in a laboratory setting.[1]

3 Results

The ability to use realistic scene geometry with chemical properties assigned by particle size enabled the simulation of an intimately mixed complex soil signature. To tune the DIRSIG born signature to match *in situ* measurements, the particle scene was systematically altered by gradually removing fine particles from the larger sand grains. A scene with large particles that are completely covered with small fines should produce a spectral emissivity curve that looks similar to the emissivity of 50 μm particles. This was accurately simulated using DIRSIG. As the fines were removed (Fig. 5), the material properties of the larger particles were shown to have a greater impact on the overall spectral signature of the mixed soil target. The desired scene geometry is the one that most closely represents the geometry and signature of disturbed soil.

A chart presenting the resulting emissivity signatures of this iterative process is shown in Fig. 6. In the figure, the curve denoted as fully covered was simulated using large particles that are entirely covered with bits of dust [Fig. 5(a)]. Between 944 and 1842 small grains were aligned to each larger particle in the scene corresponding to Fig. 5(a). Some dust was removed in the scene of particles that were less covered [Fig. 5(b)]. Between 497 and 987 small particles were aligned to each larger particle in Fig. 5(b). Even more fine grains were removed in the scene of sparsely covered particles. Between 397 and 597 small particles were aligned to individual large grains in Fig. 5(c). The total particle count for each of the three scenes ranged from 87 to 424 million particles. The sensor reaching radiance was calculated using DIRSIG 4.6.0, on a single threaded Intel® Xeon® CPU E5-2630. This machine is clocked at 2.3 GHz and has 192 GB of RAM. Run times for scenes (a–c) were approximately 10 min. The relative spectral emissivity curve of sparsely covered particles [Fig. 5(c)] is very similar to the signature of disturbed soil presented in the literature.[1] Results from this simulation also showed an increased spectral contrast and lower relative intensity in the 8 to 9.5 μm spectral band compared to scenes dominated by finely powdered quartz.[8,10]

Analytical evaluation of Fig. 6 reveals that simulation results agree with the expected theoretical balance between surface reflection and volume transmission. The Christensen

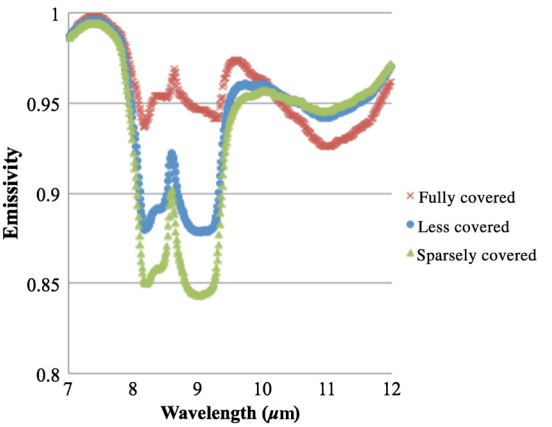

Fig. 6 Emissivity is modeled with varying amounts of clinging fines. The Scene 1 curve (red) corresponds to a geometric representation of soil particles that are completely covered with microfines. The shape and magnitude of the reststrahlen band troughs changes as microfines are gradually removed from the target scene in Scene 2 (blue) and Scene 3 (green).

frequency of quartz emerges at approximately 7.4 μm. This frequency is a benchmark because it defines nearly complete volume transmission. In this frequency region, the real part of the complex index of refraction of quartz approaches one. Air also has an index of refraction of approximately one at this wavelength. The result is the effective absence of grain boundaries. This distinct spectral feature is evident at 7.5 μm in Fig. 6.

The impact of particle size in the reststrahlen bands has been modeled with great difficulty in the past.[10] In the 8 to 9.5 μm region characterized by primary reststrahlen effects, quartz is defined by a large imaginary component of its complex index of refraction. This means that radiation is subjected to many Fresnel reflections at these wavelengths. It also implies that energy cannot easily pass through quartz grains. Therefore, two substantial troughs define emissivity in this spectral region. It has been observed that smaller grains in this region emit at higher levels than do larger quartz particles.[1,8,10] Both Salisbury and Moersch attribute this trend to the increase in volume scatter that is sensed at the top layer of a target.[8,10] Moersch explains that there are more prereabsorption interactions between thermal radiation and grain boundaries in small particles. More

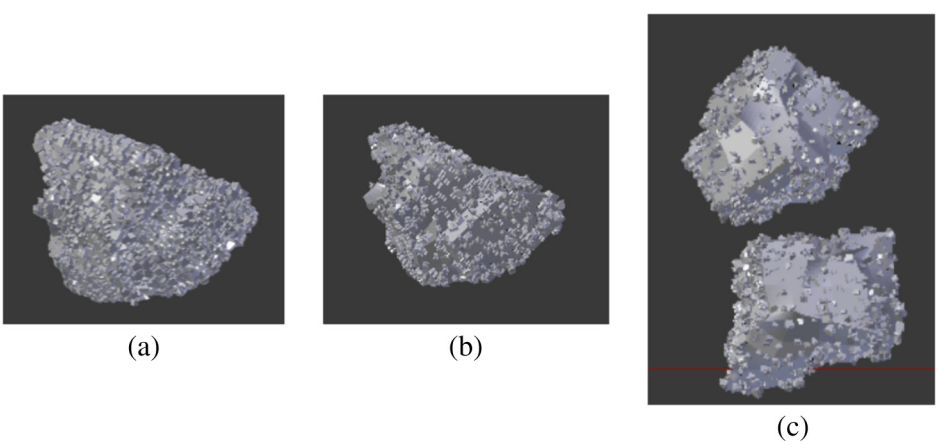

Fig. 5 (a) Particles are fully covered in clinging fines. (b) Large particles are covered less and (c) sparsely covered. The emissivity curves that correspond to these changing particle configurations show how signature varies with target geometry.

interactions translate into more opportunities for emission in this wavelength range. Figure 6 shows that the presence of clinging fine particles at the sample surface impacts the modeled signature as expected. Evidence of volume scatter in scenes of completely covered grains is evident in the flattened troughs of the reststrahlen bands. Decreased spectral contrast in this region of the curve also highlights the increased porosity and volume scatter that accompany small quartz particles. The reststrahlen region of the curve defined by sparsely covered quartz is a close match in magnitude and spectral contrast to the disturbed soil, as observed by Johnson et al.[1]

Between 10 μm and 12 μm, both volume transmission and Fresnel reflection occur in quartz. The imaginary portion of the index of refraction is very small and the real coefficient is approximately equal to two. Because volume transmission is significant in this regime, reabsorption is minimized in larger grains. This was not true in the 8 to 9.5 μm region. Since reabsorption is low, larger particles exhibit higher levels of emissivity than do small particles. As stated above, radiation from smaller particles must pass many grain boundaries before it is measured by a sensor. In the primary reststrahlen bands, this characteristic made small particles more emissive than larger particles because reabsorption was prevalent. In the 10 to 12 μm band, this very same characteristic is the purpose for lower emission levels displayed by smaller particles. This trend is described with accuracy in Fig. 6. The emissivity curves of less covered and sparsely covered soil are impacted by the presence of large soil grains. The spectral signature of the scene of completely covered grains is almost entirely characterized by fine grains. Within the 10 to 12 μm band, comparatively, higher emissivity levels should be observed in simulation results corresponding to the scenes of less covered and sparsely covered grains. This is demonstrated by this simulation approach.

4 Conclusion

The magnitude and spectral contrast signatures of quartz soil emissivity can be accurately realized only if scene geometry, radiometry, and chemistry are known. This work established that using known software tools, including Blender 3-D and DIRSIG, one can successfully model the complex mixture of disturbed soil. By incorporating the physical relationship between particle geometry and intimate mixing, known spectral features of quartz soil were tuned with precision. Spectral behavior at the Christensen frequency and the primary and secondary reststrahlen bands was correctly modeled with respect to particle size distribution. It is the ability to focus on geometric modeling that separates this technique from other models. Because DIRSIG provides complete user control of sample geometry and the assignment of spectral properties, it serves as a convenient testbed for target construction and target signature sensing. This technique can be easily modified for implementation with other material mixtures provided that pure spectral reflectance or emissivity data is available. Ultimately, this study demonstrated that by combining realistic target geometry and spectral measurements of pure quartz, emissivity of complex soil mixtures could be modeled without functional data fitting or rigorous analysis of material dynamics.

Acknowledgments

The views expressed in this article are those of the authors and do not reflect the official policy or position of the United States Air Force, Department of Defense, or the United States Government.

References

1. J. R. Johnson et al., "Infrared measurements of pristine and disturbed soils 1. Spectral contrast differences between field and laboratory data," *Remote Sens. Environ.* **64**, 34–46 (1998).
2. J. M. Cathcart et al., "Verification of a LWIR hyperspectral landmine model," *Proc. SPIE* **5415**, 1130–1139 (2004).
3. C. A. Hibbits, "Optical signatures of buried mines," in *Imaging for Detection and Identification*, pp. 49–61 (2007).
4. J. R. Johnson, P. R. Christensen, and P. G. Lucey, "Dust coatings on basaltic rocks and implications for thermal infrared spectroscopy of Mars," *J. Geophys. Res.* **107**, E6 (2002).
5. G. Koh, E. M. Winter, and M. A. Schatten, "Rainfall degradation of LWIR disturbed soil signature," *Proc. SPIE* **6217**, 62170G (2006).
6. J. Salisbury and D. M. D'Aria, "Emissivity of terrestrial materials in the 8-14m atmospheric window," *Remote Sens. Environ.* **42**(2), 83–106 (1992).
7. R. J. P. Lyon, "Evaluation of Infrared spectrophotometry for compositional analysis of lunar and planetary soils," NASA-CR-100, NASA Technical report (1964).
8. J. Salisbury and A. Wald, "The role of volume scattering in reducing spectral contrast of reststrahlen bands in spectra of powdered minerals," *Icarus* **96**, 121–128 (1992).
9. C. M. Bachmann et al., "Phase angle dependence of sand density observable in hyperspectral reflectance," *Remote Sens. Environ.* **150**, 53–65 (2014).
10. J. E. Moersch and P. R. Christensen, "Thermal emission from particulate surfaces: a comparison of scattering models with measured spectra," *J. Geophys. Res.* **100**(E4), 7465–7477 (1995).
11. B. Hapke, *Theory of Reflectance and Emittance Spectroscopy*, Cambridge University Press, Cambridge, United Kingdom (2012).
12. J. R. Maxwell et al., *Bidirectional Reflectance Model Validation and Utilization*, Environmental Research Inst. of Michigan, Ann Arbor, Michigan, 196400-1-T, (1973).
13. J. R. Schott, R. V. Raqueno, and C. Salvaggio, "Incorporation of a time-dependent thermodynamic model and a radiation propagation model into IR 3D synthetic image generation," *Opt. Eng.* **31**(7), 1505–1516 (1992).
14. J. R. Schott et al., "An advanced synthetic image generation model and its application to multi/hyperspectral algorithm development," *Can. J. Remote Sens.* **25**(2), 99–111 (1999).
15. http://www.cis.rit.edu/~cnspci/media/publications/video/spie9461-62_figure1.php.
16. J. E. Simms et al., *Analysis of Long Wave Infrared (LWIR) Soil Data to Predict Reflectance Response*, Engineer Research and Development Center Geotechnical and Structures Lab, Vicksburg, Mississippi, ERDC/GSL-TR-09-25 (2009).
17. J. P. Kerekes, K. E. Strackerjan, and C. Salvaggio, "Spectral reflectance and emissivity of man-made surfaces contaminated with environmental effects," *Opt. Eng.* **47**(10), 106201 (2008).
18. C. Salvaggio and C. J. Miller, "Methodologies and protocols for the collection of midwave and longwave infrared emissivity spectra using a portable field spectrometer," *Proc. SPIE* **4381**, 539–548 (2001).

Tyler Carson is a PhD candidate at the Rochester Institute of Technology. He received his BS degree in physics from the University of Northern Colorado and gained an Air Force commission through ROTC in 2009. He received his MS degree from the University of New Mexico Optical Science and Engineering program. He has worked previously at the Air Force Research Laboratory, where he developed solid-state lasers and optically pumped semiconductor laser devices.

Carl Salvaggio received his BS and MS degrees in imaging science from the Rochester Institute of Technology (RIT) in 1987. He received his PhD in environmental resource engineering in 1994 from the State University of New York, College of Environmental Science and Forestry, at Syracuse University. From 1994 to 2002, he worked on model validation and database development for the defense intelligence community. Since 2002 he has been a professor of imaging science at RIT.